

# Low-Cost Bayesian Inference for Additive Approximate Gaussian Process

Pulong Ma\*, Bledar A. Konomi†, and Emily L. Kang‡

Department of Mathematical Sciences, University of Cincinnati

## Abstract

Gaussian process models have been widely used in spatial/spatio-temporal statistics and uncertainty quantification. The use of a separable covariance function in these cases has computational advantages, but it ignores the potential interaction among space/time and input/output variables. In this paper we propose an additive covariance function approximation to allow for the interaction among variables in the resulting Gaussian process. The proposed method approximates the covariance function through two distinct components: a computational-complexity-reduction covariance function and a separable covariance function. The first component captures the large scale non-separable variation while the second component captures the separable variation. As shown in this paper, the new covariance structure can greatly improve the predictive accuracy but loses the computational advantages of its two distinct components. To alleviate this computational difficulty, we develop a fully conditional Markov chain Monte Carlo algorithm based on the hierarchical representation of the model. The computational cost of this algorithm is equivalent to the additive cost from the two components. The computational and inferential benefits of this new additive approximation approach are demonstrated with synthetic examples and Eastern U.S. ozone data.

*Keywords:* Additive model; Bayesian inference; Gaussian process; Metropolis-within-Gibbs sampler; nonseparable covariance function; spatio-temporal data

---

\*mapn@mail.uc.edu

†alex.konomi@uc.edu

‡kangel@ucmail.uc.edu

# 1 Introduction

Gaussian process (GP) models have been a popular instrument to model observations from geophysical and environmental studies (Cressie, 1993) as well as in uncertainty quantification, where they are used to build surrogate models for computer experiments and for model calibration (see, e.g., Sacks et al., 1989; Currin et al., 1991; Oakley and O'Hagan, 2002; Conti and O'Hagan, 2010; Konomi et al., 2014). Bayesian inference is often adopted when a GP is fitted, since it allows for a coherent inference procedure in which uncertainties from parameter estimation are also taken into account. When the size of data is large, direct implementation of a GP model usually leads to formidable computational challenge, due to the computation to invert the  $n$ -by- $n$  covariance matrix of  $n$  data points and the memory to store this covariance matrix (see, e.g., Rasmussen and Williams, 2006; Cressie and Wikle, 2011; Banerjee et al., 2014). Recently, various methods have been proposed to tackle this issue to reduce computational complexity in GP modeling for large or massive spatial data, including low-rank methods (Banerjee et al., 2008; Cressie and Johannesson, 2008; Finley et al., 2009), approximate likelihood methods (e.g., Stein et al., 2004; Gramacy and Apley, 2015), Gaussian Markov random fields (Lindgren et al., 2011), multiresolutional models (Nychka et al., 2002, 2015; Katzfuss, 2017), full-scale approximation (Sang and Huang, 2012), and the nearest neighbor Gaussian process (Datta et al., 2016a). Generally speaking, these methods take advantages of a low-rank model, a low-order conditioning set, or assumptions of a sparse covariance or precision matrix, in order to alleviate the computational difficulty of GP modeling.

In this paper, rather than considering solely geographical spatial data, we utilize the more general definition of the input and output spaces as in computer experiments, in which the input/output variables can be space, time, and/or a set of variables in the design space to be specified in order to run a computer experiment. Spatio-temporal data analysis thus can be viewed as a special case under this multiple-input/output framework. Some computational-complexity-reduction methods for spatial data have been extended for the spatio-temporal context. For example, full-scale approximation (Sang and Huang, 2012) is extended to analyze spatio-temporal dataset (Zhang et al., 2015b) and multivariate computer model outputs (Zhang et al., 2015a). The nearest neighbor Gaussian process (NNGP,

Datta et al., 2016a) is extended to analyze spatio-temporal dataset in Datta et al. (2016b). These methods pre-specify a parametric nonseparable space-time covariance function, and use various techniques to efficiently approximate the resulting GP with this covariance function. In computer experiments, when dealing with multiple input/output spaces, it is common to impose separability on the covariance function among input/output variables to reduce the number of parameters and to facilitate fast computation, although the underlying dependence structure may not be entirely separable among all variables (e.g., Conti and O'Hagan, 2010; Bilionis et al., 2013; Gramacy et al., 2015).

We propose a Gaussian process whose covariance function is approximated with an additive form from two components. The first component is nonseparable and constructed using a computational-complexity-reduction method aforementioned, while the second component assumes a separable covariance structure that increases the modeling flexibility and describes the potential separability among input/output variables. We call the resulting method the *additive approximate Gaussian process* (AAGP), since its additive form of covariance functions can approximate any type of target covariance function, separable or nonseparable, in terms of its implied dependence structure, in a data-driven way. On the methodological end, although our method, AAGP, inherits the additive modeling form as some other methods such as the modified predictive process (MPP, Finley et al., 2009), the full scale approximation (FSA, Sang and Huang, 2012), and the multi-resolution approximation (MRA, Katzfuss, 2017), our method differs from these methods substantially in the sense that they use multiple components altogether to approximate a single parametric covariance function. Rather, our method uses two different components to model different dependence structures, respectively. As demonstrated by numerical studies, our method is robust and flexible since it allows data to determine how much variation is explained by these two components, respectively, instead of simply assuming a covariance function that is either separable or nonseparable. Moreover, although we use MPP as the computational-complexity-reduction component of AAGP in numerical illustrations, the AAGP framework and the associated computational procedure are general and applicable if a different computational-complexity-reduction method, such as FSA, MRA, or NNGP, is chosen for this component of AAGP. To avoid computational complexity, we use in this

paper the MPP as a first approximation component.

Our method also differs from previous methods using an additive structure resulting from two different covariance components. Rougier (2008) uses a low-rank component plus a separable covariance function while the low-rank component is constructed with pre-specified regressors of input/output variables in a separable form. Our method explicitly includes the nonseparable dependence structure into the model which is not necessarily low-rank. In addition, our model includes a nugget term recommended in Gramacy and Lee (2012) and Peng and Wu (2014), to ensure computational stability and better prediction performances. Ma and Kang (2017) propose a model with a low-rank component and a Gaussian graphical model that induces a sparse precision matrix, but their method applies to spatial data instead of data from multiple-input/output space in general. One more example for an additive covariance function model is the work in Ba and Joseph (2012). They model a process as a sum of two independent GPs with separable squared exponential covariance functions, and have to impose empirical constraints on parameters in these two covariance functions to avoid non-identifiability. Our method avoids such an issue by using different types of covariance structure for the two components and is designed to handle large datasets in a Bayesian framework.

Conventional likelihood-based or fully Bayesian inference procedures for GP modeling typically focus on the marginalized model after integrating out random effects in the GPs (e.g., Ba and Joseph, 2012; Banerjee et al., 2014). With large datasets, such an inference procedure usually relies on the Sherman-Morrison-Woodbury formula (Henderson and Searle, 1981) or the Cholesky decomposition of a sparse matrix to reduce computational complexity (Sang and Huang, 2012; Datta et al., 2016a; Katzfuss, 2017). For AAGP, we show that these techniques cannot alleviate any computational burden, and that direct inference from the marginalized model is computationally infeasible. Instead, we propose a fully conditional Markov chain Monte Carlo (MCMC) algorithm to enable fast Bayesian inference for large datasets when a covariance function admits an additive form of multiple components. Choosing MPP as the computational-complexity-reduction component in AAGP, we demonstrate the computational advantages of this inference procedure with synthetic examples and real data. Meanwhile, we describe how this efficient Bayesian in-

ference procedure can be applied in general if a different method such as FSA, MRA, or NNGP is utilized as the computational-complexity-reduction component in AAGP.

The remainder of this paper is organized as follows. Section 2 presents the basic definition of the additive approximate Gaussian process and its covariance function specification. Section 3 gives details about the fast Metropolis-within-Gibbs sampler based on the fully hierarchical formulation of the AAGP model, and its extension with other covariance specifications in AAGP. Section 4 illustrates the predictive performance of AAGP with simulation examples and real data analysis. Section 5 concludes with discussions on possible extensions.

## 2 The Additive Approximate Gaussian Process Model

Assume that we observe the response at a total of  $n$  inputs,  $\mathbf{x}_1, \dots, \mathbf{x}_n \in \mathcal{X}$ . The corresponding observations are denoted by  $Z(\mathbf{x}_1), \dots, Z(\mathbf{x}_n)$ . We assume the following model for  $Z(\cdot)$ :

$$Z(\mathbf{x}) = Y(\mathbf{x}) + \epsilon(\mathbf{x}), \mathbf{x} \in \mathcal{X}, \quad (2.1)$$

where  $Y(\cdot)$  is a latent Gaussian process of interest. The second term in the right-hand side,  $\epsilon(\cdot)$ , is assumed to be a Gaussian white noise with variance  $\tau^2$ , which is usually called the nugget effect. This term is commonly used to represent measurement errors when analyzing environmental data, but is also recommended when analyzing computer experiment outputs to ensure computational stability and robust prediction accuracy although the outputs from a computer experiment are deterministic (Gramacy and Lee, 2012; Peng and Wu, 2014).

The process  $Y(\cdot)$  is usually assumed to have additive components:

$$Y(\mathbf{x}) = \mathbf{h}(\mathbf{x})^T \mathbf{b} + w(\mathbf{x}), \mathbf{x} \in \mathcal{X}, \quad (2.2)$$

where  $\mathbf{h}(\cdot) = [h_1(\cdot), h_1(\cdot), \dots, h_p(\cdot)]^T$  is a vector of  $p$  covariates;  $\mathbf{b}$  is the corresponding vector of  $p$  regression coefficients;  $w(\cdot)$  is a Gaussian process with mean zero and covariance function  $C(\cdot, \cdot)$ . To reduce the computational complexity but also to increase flexibility

in the dependence structure we assume that the process  $w(\cdot)$  is approximated with the summation of two computationally efficient components  $w_1(\cdot)$  and  $w_2(\cdot)$ . We assume that  $w_1(\cdot)$  and  $w_2(\cdot)$  are independent Gaussian processes and have two different covariance functions families,  $C_1(\cdot, \cdot)$  and  $C_2(\cdot, \cdot)$  respectively. We call the resulting process  $Y(\cdot) = \mathbf{h}(\mathbf{x})^T \mathbf{b} + w_1(\mathbf{x}) + w_2(\mathbf{x})$  the additive approximate Gaussian process (AAGP). Its covariance function can be written as  $\text{cov}(Y(\mathbf{x}), Y(\mathbf{x}')) = C_1(\mathbf{x}, \mathbf{x}') + C_2(\mathbf{x}, \mathbf{x}')$  with the two components  $C_1(\cdot, \cdot)$  and  $C_2(\cdot, \cdot)$  described below.

In this paper we concentrate into two specific forms of the covariance functions. We choose a nonseparable low rank covariance function  $C_1(\cdot, \cdot)$ , the modified predictive process, and a separable one  $C_2(\cdot, \cdot)$  in AAGP. The choice of using a nonseparable correlation function avoids the non-identifiability issue since these covariance functions characterize different dependence structures. Therefore, unlike imposing empirically strict constraints on parameters in Ba and Joseph (2012), our model can be fit in a purely data-driven way. Secondly, as demonstrated by numerical examples in Section 4, with both of the computationally efficient nonseparable and separable components, AAGP is more flexible to model various dependence structure and gives robust predictive performance. Finally, AAGP consists of two different covariance components, which is fundamentally different from methods such as FSA and MRA in essence, because those methods are designed to use multiple components altogether to approximate a single covariance function. Actually, both FSA and MRA are alternative computational-complexity-reduction methods to model the component  $w_1(\cdot)$  in AAGP.

**First Component - Modified Predictive Process:** To deal with large data size  $n$ , we adopt an approximation method to reduce computational complexity resulting from  $w_1(\cdot)$  with the nonseparable covariance function  $C_1(\cdot, \cdot)$ . Predictive process methods (e.g., Banerjee et al., 2008; Finley et al., 2009) have been proposed and applied successfully with large data. These methods assume models with reduced dimension and require only linear computational cost to invert large covariance matrix via applying the Sherman-Morrison-Woodbury formula. Specifically, we assume a nonseparable correlation function  $R_0(\cdot, \cdot; \boldsymbol{\theta}_1)$  known up to a few parameters  $\boldsymbol{\theta}_1$ . Pre-specifying a set of  $m$  ( $m \ll n$ ) knots  $\mathcal{X}^* \equiv \{\mathbf{x}_1^*, \dots, \mathbf{x}_m^*\} \subset \mathcal{X}$ , we model the process  $w_1(\cdot)$  as a GP with mean zero and correlation

function given by:

$$R_1(\mathbf{x}, \mathbf{x}') = \mathbf{R}(\mathbf{x}, \mathcal{X}^*) \mathbf{R}_*^{-1} \mathbf{R}(\mathbf{x}', \mathcal{X}^*)^T + I(\mathbf{x} = \mathbf{x}') [1 - \mathbf{R}(\mathbf{x}, \mathcal{X}^*) \mathbf{R}_*^{-1} \mathbf{R}(\mathbf{x}', \mathcal{X}^*)^T],$$

where  $\mathbf{R}(\mathbf{x}, \mathcal{X}^*) \equiv [R_0(\mathbf{x}, \mathbf{x}_i^*)]_{i=1, \dots, m}$  is an  $m$ -dimensional row vector;  $\mathbf{R}_*$  is the  $m$ -by- $m$  matrix with its  $(i, j)$ -th element  $R_0(\mathbf{x}_i^*, \mathbf{x}_j^*)$ , for  $i, j = 1, \dots, m$ , and  $I(\cdot)$  denotes the indicator function of its argument. It is straightforward that  $R_1(\mathbf{x}, \mathbf{x}') = 1$  if  $\mathbf{x} = \mathbf{x}'$ . Considering the  $n$ -dimensional vector corresponding to the  $n$  design locations with observations,  $\mathbf{w}_1 \equiv (w_1(\mathbf{x}_1), \dots, w_1(\mathbf{x}_n))^T$ , its correlation matrix is  $\mathbf{R}_1 \equiv \mathbf{R}_{nm} \mathbf{R}_*^{-1} \mathbf{R}_{nm}^T + \mathbf{V}$ , where  $\mathbf{R}_{nm} \equiv [R_0(\mathbf{x}_i, \mathbf{x}_j^*)]_{i=1, \dots, n; j=1, \dots, m}$ , and  $\mathbf{V}$  is an  $n$ -by- $n$  diagonal matrix with its  $i$ th diagonal element given by  $V_i \equiv 1 - \mathbf{R}(\mathbf{x}_i, \mathcal{X}^*) \mathbf{R}_*^{-1} \mathbf{R}(\mathbf{x}_i, \mathcal{X}^*)^T$ , for  $i = 1, \dots, n$ . Note that the vector  $\mathbf{R}(\mathbf{x}, \mathcal{X}^*)$  and matrices  $\mathbf{R}_*$  and  $\mathbf{V}$  all depend on the unknown parameters  $\boldsymbol{\theta}_1$ . The resulting covariance function  $C_1(\cdot, \cdot; \boldsymbol{\theta}_1)$  is  $\sigma_1^2 R_1(\cdot, \cdot; \boldsymbol{\theta}_1)$ , where  $\sigma_1^2$  is a variance parameter. Readers are referred to Finley et al. (2009) for more details on MPP. Although we demonstrate AAGP using MPP as the computational-complexity-reduction method for the nonseparable component in all numerical examples, we discuss in Section 3 on how the general inference procedure will apply if a different method, such as FSA, NNGP, or MRA, is adopted for  $w_1(\cdot)$ .

**Second Component - Separable model:** We assume a separable covariance function for the process  $w_2(\cdot)$ . Without loss of generality, we represent the space of design locations,  $\mathcal{X}$ , as a product space  $\mathcal{X}_1 \times \mathcal{X}_2$ , and assume that  $C_2(\mathbf{x}, \mathbf{x}'; \boldsymbol{\theta}_2) = \sigma_2^2 \rho_1(\mathbf{s}, \mathbf{s}'; \boldsymbol{\phi}_1) \rho_2(\mathbf{u}, \mathbf{u}'; \boldsymbol{\phi}_2)$  for  $\mathbf{s}, \mathbf{s}' \in \mathcal{X}_1$ ,  $\mathbf{u}, \mathbf{u}' \in \mathcal{X}_2$ ,  $\mathbf{x} = (\mathbf{s}, \mathbf{u}) \in \mathcal{X}$ , and  $\mathbf{x}' = (\mathbf{s}', \mathbf{u}') \in \mathcal{X}$ . Here,  $\rho_1(\cdot, \cdot)$  and  $\rho_2(\cdot, \cdot)$  are correlation functions with parameters  $\boldsymbol{\phi}_1$  and  $\boldsymbol{\phi}_2$ , respectively and thus the unknown parameters associated with  $w_2(\cdot)$  are  $\sigma_2^2$  and  $\boldsymbol{\theta}_2 = \{\boldsymbol{\phi}_1, \boldsymbol{\phi}_2\}$ . The parameter  $\sigma_2^2$  is a variance parameter. For the present, the response  $Z$  is assumed to be observed at all the  $n = n_1 n_2$  design locations arranged as  $\mathbf{x}_1 = (\mathbf{s}_1, \mathbf{u}_1), \dots, \mathbf{x}_{n_2} = (\mathbf{s}_1, \mathbf{u}_{n_2}), \mathbf{x}_{n_2+1} = (\mathbf{s}_2, \mathbf{u}_1), \dots, \mathbf{x}_{2n_2} = (\mathbf{s}_2, \mathbf{u}_{n_2}), \dots, \mathbf{x}_n = (\mathbf{s}_{n_1}, \mathbf{u}_{n_2})$ , where  $n_1$  denotes the number of locations in  $\mathcal{X}_1$ , and  $n_2$  denotes that in  $\mathcal{X}_2$ . The locations  $\{\mathbf{s}_1, \dots, \mathbf{s}_{n_1}\}$  and  $\{\mathbf{u}_1, \dots, \mathbf{u}_{n_2}\}$  are not necessarily regularly spread out in  $\mathcal{X}_1$  and  $\mathcal{X}_2$ . The resulting correlation matrix of  $\mathbf{w}_2 \equiv (w_2(\mathbf{x}_1), \dots, w_2(\mathbf{x}_n))^T$  is  $\mathbf{R}_2 \equiv \mathbf{R}_s \otimes \mathbf{R}_u$ , where  $\mathbf{R}_s \equiv [\rho_1(\mathbf{s}_i, \mathbf{s}_j)]_{i,j=1, \dots, n_1}$  is an  $n_1$ -

by- $n_1$  matrix, and  $\mathbf{R}_u \equiv [\rho_2(\mathbf{u}_i, \mathbf{u}_j)]_{i,j=1,\dots,n_2}$  is an  $n_2$ -by- $n_2$  matrix. As shown in Genton (2007) and Rougier (2008), imposing separability on the covariance function enables us to use attractive properties of Kronecker product of matrices, which brings substantial computational gains to calculations associated with  $C_2(\cdot, \cdot)$ . The tentative assumption that  $Z$  is observed at all the  $n = n_1 n_2$  design locations is relaxed in Section 3.4, and we describe there how missing data imputation is carried out in the Bayesian inference.

**Likelihood:** Let  $\mathbf{Z} \equiv (Z(\mathbf{x}_1), \dots, Z(\mathbf{x}_n))^T$  be the  $n$ -dimensional vector of observations. Given the model and the covariance structure, as specified above, we can write the log likelihood of the data vector  $\mathbf{Z}$  as:

$$\ell(\mathbf{b}, \tau^2, \sigma_1^2, \sigma_2^2, \boldsymbol{\theta}_1, \boldsymbol{\theta}_2; \mathbf{Z}) = -n \log(2\pi)/2 - \log(|\boldsymbol{\Sigma}|)/2 - (\mathbf{Z} - \mathbf{H}\mathbf{b})^T \boldsymbol{\Sigma}^{-1} (\mathbf{Z} - \mathbf{H}\mathbf{b})/2 \quad (2.3)$$

where  $\mathbf{H} \equiv [\mathbf{h}(\mathbf{x}_1), \dots, \mathbf{h}(\mathbf{x}_n)]^T$  the matrix with the basis functions, and  $\boldsymbol{\Sigma}$  is the covariance matrix of  $\mathbf{Z}$  :

$$\begin{aligned} \boldsymbol{\Sigma} &\equiv \text{cov}(\mathbf{Z}) = \sigma_1^2 \mathbf{R}_1 + \sigma_2^2 \mathbf{R}_s \otimes \mathbf{R}_u + \tau^2 \mathbf{I}, \\ &= \sigma_1^2 \mathbf{R}_{nm} \mathbf{R}_*^{-1} \mathbf{R}_{nm}^T + \sigma_2^2 \mathbf{R}_s \otimes \mathbf{R}_u + \sigma_1^2 \mathbf{V} + \tau^2 \mathbf{I}. \end{aligned} \quad (2.4)$$

Evaluation of this function involves the inversion and log-determinant of the  $n$ -by- $n$  covariance matrix  $\boldsymbol{\Sigma}$ . With large  $n$ , the Sherman-Morrison-Woodbury formula or the Cholesky decomposition of sparse matrices have been suggested to reduce computational complexity (Sang and Huang, 2012; Datta et al., 2016a; Katzfuss, 2017). However, these techniques cannot reduce computational complexity for AAGP and calculations related to the matrix  $\boldsymbol{\Sigma}$ . Specifically, let  $\mathbf{D} \equiv \sigma_2^2 \mathbf{R}_s \otimes \mathbf{R}_u + \sigma_1^2 \mathbf{V} + \tau^2 \mathbf{I}$ . Although we can then use the Sherman-Morrison-Woodbury formula to obtain that  $\boldsymbol{\Sigma}^{-1} = \mathbf{D}^{-1} - \mathbf{D}^{-1} \mathbf{R}_{nm} [\mathbf{R}_*/\sigma_1^2 + \mathbf{R}_{nm}^T (\mathbf{R}_*/\sigma_1^2)^{-1} \mathbf{R}_{nm}]^{-1} \mathbf{R}_{nm}^T \mathbf{D}^{-1}$ , it should be noted that calculating this inversion  $\boldsymbol{\Sigma}^{-1}$  is not computationally feasible. In particular, it requires inversions of two  $m$ -by- $m$  matrices,  $\mathbf{R}_*$  and  $\mathbf{R}_*/\sigma_1^2 + \mathbf{R}_{nm} (\mathbf{R}_*/\sigma_1^2)^{-1} \mathbf{R}_{nm}$ , and inversion of the  $n$ -by- $n$  matrix  $\mathbf{D}$ . As  $m$  is much smaller than  $n$ , inverting the  $m$ -by- $m$  matrices can be done easily with  $O(m^3)$  flops since we have  $m$  much smaller than  $n$ . However, inverting the  $n$ -by- $n$  matrix  $\mathbf{D}$  requires full

matrix inversion due to the presence of heterogeneous diagonal elements in  $\sigma_1^2 \mathbf{V}$ , and thus costs  $O(n^3)$  flops and  $O(n^2)$  memory. Bayesian inference based on the marginalized form of the likelihood above is computationally expensive with  $O(n^3)$  flops and  $O(n^2)$  memory in each iteration of the Markov chain Monte Carlo method. To overcome this difficulty, we base our inference on the conditional form of the likelihood and develop an efficient Metropolis-within-Gibbs sampler for AAGP in Section 3.1, which allows for fast Bayesian inference with large datasets.

### 3 Bayesian Inference

To carry out Bayesian inference for in AAGP, we first assign priors distributions to the unknown parameters  $\{\mathbf{b}, \tau^2, \sigma_1^2, \sigma_2^2, \boldsymbol{\theta}_1, \boldsymbol{\theta}_2\}$ . Following customary prior specifications, we assign a vague multivariate normal prior to the coefficient vector  $\mathbf{b} \sim \mathcal{N}_p(\boldsymbol{\mu}_b, \mathbf{V}_b)$ ; inverse gamma priors are assigned to variance parameters,  $\tau^2 \sim \mathcal{IG}(a_\tau, b_\tau)$ ,  $\sigma_1^2 \sim \mathcal{IG}(a_1, b_1)$ , and  $\sigma_2^2 \sim \mathcal{IG}(a_2, b_2)$ ; other covariance parameters in  $\boldsymbol{\theta}_1$  and  $\boldsymbol{\theta}_2$  such as range parameters are assigned with uniform priors.

Conventional fully Bayesian inference procedures for GP modeling typically focus the marginalized model after integrating out random effects, and obtain posterior distribution of unknown parameters given data. For AAGP, we can write out the (joint) posterior distribution  $p(\mathbf{b}, \tau^2, \sigma_1^2, \sigma_2^2, \boldsymbol{\theta}_1, \boldsymbol{\theta}_2 | \mathbf{Z})$ , which is proportional to the joint distribution:

$$\begin{aligned} & p(\mathbf{b}, \tau^2, \sigma_1^2, \sigma_2^2, \boldsymbol{\theta}_1, \boldsymbol{\theta}_2) p(\mathbf{Z} | \mathbf{b}, \tau^2, \sigma_1^2, \sigma_2^2, \boldsymbol{\theta}_1, \boldsymbol{\theta}_2) \\ &= \mathcal{N}_p(\boldsymbol{\mu}_b, \mathbf{V}_b) \mathcal{IG}(a_\tau, b_\tau) \mathcal{IG}(a_1, b_1) \mathcal{IG}(a_2, b_2) p(\boldsymbol{\theta}_1, \boldsymbol{\theta}_2) \times \mathcal{N}_n(\mathbf{H}\mathbf{b}, \boldsymbol{\Sigma}). \end{aligned} \quad (3.1)$$

Sampling from this posterior distribution (3.1) is computationally infeasible with large  $n$ , since each MCMC iteration requires inversion of the  $n \times n$  covariance matrix  $\boldsymbol{\Sigma}$  and hence costs  $O(n^3)$  flops and  $O(n^2)$  memory to compute the likelihood. Here, rather than utilizing the marginal distribution of  $\mathbf{Z}$ , we write the model in a hierarchical form of AAGP involving the latent processes  $w_1(\cdot)$  and  $w_2(\cdot)$ , based on which we propose a computationally efficient MCMC sampler.

The models (2.1) and (2.2) can be written as follows to give a hierarchical formulation

of AAGP:

$$\mathbf{Z} \mid \mathbf{b}, \mathbf{w}_1, \mathbf{w}_2, \tau^2 \sim \mathcal{N}_n(\mathbf{Hb} + \mathbf{w}_1 + \mathbf{w}_2, \tau^2 \mathbf{I}_n), \quad (3.2)$$

$$\mathbf{w}_1 \mid \sigma_1^2, \boldsymbol{\theta}_1 \sim \mathcal{N}_n(\mathbf{R}_{nm} \mathbf{R}_*^{-1} \mathbf{w}^*, \sigma_1^2 \mathbf{V}), \quad (3.3)$$

$$\mathbf{w}_2 \mid \sigma_2^2, \boldsymbol{\theta}_2 \sim \mathcal{N}_n(\mathbf{0}, \sigma_2^2 \mathbf{R}_s \otimes \mathbf{R}_u), \quad (3.4)$$

where  $\mathbf{I}_n$  denotes the  $n$ -by- $n$  identity matrix, and  $\mathbf{w}^* \equiv (w_1(\mathbf{x}_1^*), \dots, w_1(\mathbf{x}_m^*))^T$  is a vector of length  $m$  following multivariate normal distribution with mean zero and covariance matrix  $\sigma_1^2 \mathbf{R}_*$ . The joint posterior distribution of all the unknowns, including both of parameters  $\{\mathbf{b}, \tau^2, \sigma_1^2, \sigma_2^2, \boldsymbol{\theta}_1, \boldsymbol{\theta}_2\}$  and latent random effects  $\mathbf{w}^*$ ,  $\mathbf{w}_1$ , and  $\mathbf{w}_2$ , can be obtained:

$$\begin{aligned} & p(\mathbf{b}, \tau^2, \sigma_1^2, \sigma_2^2, \boldsymbol{\theta}_1, \boldsymbol{\theta}_2, \mathbf{w}^*, \mathbf{w}_1, \mathbf{w}_2 \mid \mathbf{Z}) \\ & \propto \mathcal{N}_p(\boldsymbol{\mu}_b, \mathbf{V}_b) \mathcal{IG}(a_\tau, b_\tau) \mathcal{IG}(a_1, b_1) \mathcal{IG}(a_2, b_2) p(\boldsymbol{\theta}_1, \boldsymbol{\theta}_2) \\ & \quad \times \mathcal{N}_m(\mathbf{w}^* \mid \mathbf{0}, \sigma_1^2 \mathbf{R}_*) \times \mathcal{N}_n(\mathbf{w}_1 \mid \mathbf{R}_{nm} \mathbf{R}_*^{-1} \mathbf{w}^*, \sigma_1^2 \mathbf{V}) \\ & \quad \times \mathcal{N}_n(\mathbf{w}_2 \mid \mathbf{0}, \sigma_2^2 \mathbf{R}_s \otimes \mathbf{R}_u) \times \mathcal{N}_n(\mathbf{Z} \mid \mathbf{Hb} + \mathbf{w}_1 + \mathbf{w}_2, \tau^2 \mathbf{I}_n). \end{aligned} \quad (3.5)$$

### 3.1 Parameter Estimation & Computational Cost

Since the posterior distribution (3.5) is intractable, we use a Metropolis-within-Gibbs sampler (Mueller, 1993; Gelfand and Smith, 1990; Hastings, 1970) for parameter inference in the hierarchical representation of the posterior distribution. In particular, we have conjugate full conditional distributions for  $\mathbf{b}, \tau^2, \sigma_1^2, \sigma_2^2$  and multivariate normal full conditional distributions for random effects  $\mathbf{w}^*$ ,  $\mathbf{w}_1$ , and  $\mathbf{w}_2$  given below:

$$\begin{aligned} \mathbf{b} \mid \cdot & \sim \mathcal{N}_p(\boldsymbol{\mu}_{\mathbf{b}}^*, \mathbf{V}_{\mathbf{b}}^*), \\ \sigma_1^2 \mid \cdot & \sim \mathcal{IG}(a_1 + \frac{m+n}{2}, b_1 + \frac{\mathbf{w}^{*T} \mathbf{R}_*^{-1} \mathbf{w}^* + (\mathbf{w}_1 - \mathbf{R}_{nm} \mathbf{R}_*^{-1} \mathbf{w}^*)^T \mathbf{V}^{-1} (\mathbf{w}_1 - \mathbf{R}_{nm} \mathbf{R}_*^{-1} \mathbf{w}^*)}{2}), \\ \sigma_2^2 \mid \cdot & \sim \mathcal{IG}(a_2 + \frac{n}{2}, b_2 + \frac{\mathbf{w}_2^T (\mathbf{R}_s \otimes \mathbf{R}_u)^{-1} \mathbf{w}_2}{2}), \\ \tau^2 \mid \cdot & \sim \mathcal{IG}(a_\tau + \frac{n}{2}, b_\tau + \frac{(\mathbf{Z} - \mathbf{Hb} - \mathbf{w}_1 - \mathbf{w}_2)^T (\mathbf{Z} - \mathbf{Hb} - \mathbf{w}_1 - \mathbf{w}_2)}{2}), \\ \mathbf{w}^* \mid \cdot & \sim \mathcal{N}_m(\boldsymbol{\mu}_{\mathbf{w}^* \mid \cdot}, \boldsymbol{\Sigma}_{\mathbf{w}^* \mid \cdot}), \\ \mathbf{w}_1 \mid \cdot & \sim \mathcal{N}_n(\boldsymbol{\mu}_{1 \mid \cdot}, \boldsymbol{\Sigma}_{1 \mid \cdot}), \\ \mathbf{w}_2 \mid \cdot & \sim \mathcal{N}_n(\boldsymbol{\mu}_{2 \mid \cdot}, \boldsymbol{\Sigma}_{2 \mid \cdot}), \end{aligned}$$

where  $\boldsymbol{\mu}_b^* = \mathbf{V}_b^*[\tau^{-2}\mathbf{H}^T(\mathbf{Z} - \mathbf{w}_1 - \mathbf{w}_2) + \mathbf{V}_b^{-1}\boldsymbol{\mu}_b]$ , and  $\mathbf{V}_b^* = [\tau^{-2}\mathbf{H}^T\mathbf{H} + \mathbf{V}_b^{-1}]^{-1}$ ;  $\boldsymbol{\mu}_{\mathbf{w}^*| \cdot} = \boldsymbol{\Sigma}_{\mathbf{w}^*| \cdot}\mathbf{R}_*^{-1}\mathbf{R}_{nm}^T(\sigma_1^2\mathbf{V})^{-1}\mathbf{w}_1$ , and  $\boldsymbol{\Sigma}_{\mathbf{w}^*| \cdot} = \sigma_1^2(\mathbf{R}_*^{-1} + \mathbf{R}_*^{-1}\mathbf{R}_{nm}^T\mathbf{V}^{-1}\mathbf{R}_{nm}\mathbf{R}_*^{-1})^{-1} = \sigma_1^2\mathbf{R}_*(\mathbf{R}_* + \mathbf{R}_{nm}^T\mathbf{V}^{-1}\mathbf{R}_{nm})^{-1}\mathbf{R}_*^T$ ;  $\boldsymbol{\mu}_{1| \cdot} = \boldsymbol{\Sigma}_{1| \cdot}[(\sigma_1^2\mathbf{V})^{-1}\mathbf{R}_{nm}\mathbf{R}_*^{-1}\mathbf{w}^* + \tau^{-2}(\mathbf{Z} - \mathbf{Hb} - \mathbf{w}_2)]$ , and  $\boldsymbol{\Sigma}_{1| \cdot} = [\tau^{-2}\mathbf{I}_n + (\sigma_1^2\mathbf{V})^{-1}]^{-1}$ ;  $\boldsymbol{\mu}_{2| \cdot} = \tau^{-2}\boldsymbol{\Sigma}_{2| \cdot}(\mathbf{Z} - \mathbf{Hb} - \mathbf{w}_1)$ , and  $\boldsymbol{\Sigma}_{2| \cdot} = [\tau^{-2}\mathbf{I}_n + (\sigma_2^2\mathbf{R}_s \otimes \mathbf{R}_u)^{-1}]^{-1}$ .

Close inspection of these full conditional distributions  $p(\mathbf{w}^* | \cdot)$ ,  $p(\mathbf{w}_1 | \cdot)$ ,  $p(\mathbf{w}_2 | \cdot)$ ,  $p(\mathbf{b} | \cdot)$ ,  $p(\sigma_1^2 | \cdot)$ ,  $p(\sigma_2^2 | \cdot)$ ,  $p(\tau^2 | \cdot)$  reveals that sampling from them only requires inversions of  $n$ -by- $n$  diagonal matrices,  $m$ -by- $m$  low-dimensional matrices, and  $n_1$ -by- $n_1$ ,  $n_2$ -by- $n_2$  small matrices, thus making this inference procedure computationally attractive. For instance, to sample from the distribution  $[\mathbf{w}_2 | \cdot] = \mathcal{N}_n(\boldsymbol{\mu}_{2| \cdot}, \boldsymbol{\Sigma}_{2| \cdot})$ , we can obtain the eigenvalue decomposition of  $\boldsymbol{\Sigma}_{2| \cdot}$  using the properties of Kronecker product of matrices in Appendix A. Specifically, we first carry out eigenvalue decompositions for matrices  $\mathbf{R}_s = \mathbf{U}_1\boldsymbol{\Lambda}_1\mathbf{U}_1^T$  and  $\mathbf{R}_u = \mathbf{U}_2\boldsymbol{\Lambda}_2\mathbf{U}_2^T$  with computational cost  $O(n_1^3 + n_2^3)$  in total. Then with  $\boldsymbol{\zeta}$  generated as an  $n$ -dimensional vector of independent samples from the standard normal distribution, a sample from  $\mathcal{N}_n(\boldsymbol{\mu}_{2| \cdot}, \boldsymbol{\Sigma}_{2| \cdot})$  is obtained by carry out the matrix-vector multiplication,  $(\mathbf{U}_1 \otimes \mathbf{U}_2)\boldsymbol{\Lambda}^{1/2}\boldsymbol{\zeta}$ , where  $\boldsymbol{\Lambda}^{1/2}$  denotes the square root of the diagonal matrix  $(\boldsymbol{\Lambda}_1^{-1} \otimes \boldsymbol{\Lambda}_2^{-1}/\sigma_2^2 + \tau^{-2}\mathbf{I}_n)^{-1}$ . This matrix-vector multiplication requires computational cost  $O(n_1^3 + n_2^3 + n(n_1 + n_2))$  according to Eq. (A.4) and Eq. (A.6) in Appendix A.

To sample  $\boldsymbol{\theta}_1$  and  $\boldsymbol{\theta}_2$  from their full conditional distributions, a Metropolis-Hastings step is incorporated for each parameter. These full conditional distributions are not any standard distribution, but we know them up to some normalizing constant as follows:

$$p(\boldsymbol{\theta}_1 | \cdot) \propto p(\boldsymbol{\theta}_1) \times \mathcal{N}_m(\mathbf{w}^* | \mathbf{0}, \sigma_1^2\mathbf{R}_*) \times \mathcal{N}_n(\mathbf{w}_1 | \mathbf{R}_{nm}\mathbf{R}_*^{-1}\mathbf{w}^*, \sigma_1^2\mathbf{V}), \quad (3.6)$$

$$p(\boldsymbol{\theta}_2 | \cdot) \propto p(\boldsymbol{\theta}_2) \times \mathcal{N}_n(\mathbf{w}_2 | \mathbf{0}, \sigma_2^2\mathbf{R}_s \otimes \mathbf{R}_u). \quad (3.7)$$

Let  $\theta$  denote a generic scalar parameter in  $\boldsymbol{\theta}_1$  or  $\boldsymbol{\theta}_2$  with the target probability density  $\pi(\theta)$  given in Eq. (3.6) or Eq. (3.7). Let  $J(\theta^* | \theta)$  denote the proposal distribution for  $\theta$ . Then the corresponding acceptance ratio  $\alpha_0$  in the Metropolis-Hastings step for  $\theta$  is

$$\alpha_0 = \min \left\{ 1, \frac{\pi(\theta^*)J(\theta^* | \theta)}{\pi(\theta)J(\theta | \theta^*)} \right\}.$$

Let  $\mu$  be a random number generated from  $U([0, 1])$ . The proposed candidate  $\theta^*$  is accepted

if  $\alpha_0 > \mu$ ; otherwise, the proposed candidate is rejected.

The Metropolis-within-Gibbs sampler described above is computationally efficient. In terms of computational cost, sampling from the full conditional distributions of  $\mathbf{b}$ ,  $\tau^2$ ,  $\sigma_1^2$ ,  $\sigma_2^2$ ,  $\mathbf{w}^*$ ,  $\mathbf{w}_1$ , and  $\mathbf{w}_2$  requires  $O(m^3 + m^2n + n_1^3 + n_2^3 + n(n_1 + n_2))$  flops. Sampling from full conditional distributions for  $\boldsymbol{\theta}_1$  and  $\boldsymbol{\theta}_2$  requires  $O(m^3 + m^2n + n_1^3 + n_2^3 + n(n_1 + n_2))$  flops. Therefore, the overall computational cost for each MCMC iteration is  $O(m^2n + n_1^3 + n_2^3 + n(n_1 + n_2))$ . Note that  $m$ ,  $n_1$ , and  $n_2$  are all smaller than  $n$ , which makes this inference procedure much more efficient than dealing with marginalized joint density by integrating random effects. It is worth mentioning that if either  $n_1$  or  $n_2$  is large, it is desirable or even necessary to further reduce computational complexity of the current Bayesian inference procedure, and we discuss in Section 5 on how to extend AAGP and the Metropolis-within-Gibbs sampler for very large data with large  $n_1$  or  $n_2$ . Moreover, although we sample the  $n$ -dimensional vectors  $\mathbf{w}_1$  and  $\mathbf{w}_2$  in the Gibbs sampler, it is worth noting that there is no need to store all samples of these two high-dimensional vectors from all MCMC iterations, because they can always be recovered easily through  $[\mathbf{w}_1|\mathbf{Z}] = \int [\mathbf{w}_1|\sigma_1^2, \boldsymbol{\theta}_1][\sigma_1^2, \boldsymbol{\theta}_1|\mathbf{Z}] d\{\sigma_1^2, \boldsymbol{\theta}_1\}$  and  $[\mathbf{w}_2|\mathbf{Z}] = \int [\mathbf{w}_2|\sigma_2^2, \boldsymbol{\theta}_2][\sigma_2^2, \boldsymbol{\theta}_2|\mathbf{Z}] d\{\sigma_2^2, \boldsymbol{\theta}_2\}$ . Therefore, the overall memory cost for each MCMC iteration is roughly  $O(mn + n_1^2 + n_2^2)$ .

To further improve computational efficiency, the random vector  $\mathbf{w}^*$  and parameter  $\sigma_1^2$  can be integrated out when sampling from  $p(\boldsymbol{\theta}_1 | \cdot) \equiv p(\boldsymbol{\theta}_1 | \mathbf{w}_1, \mathbf{w}^*, \sigma_1^2)$ . That is, we seek the joint conditional distribution  $p(\boldsymbol{\theta}_1, \mathbf{w}^*, \sigma_1^2 | \mathbf{w}_1)$ , and then integrate out  $\mathbf{w}^*, \sigma_1^2$  to obtain the conditional distribution of  $\boldsymbol{\theta}_1$  given  $\mathbf{w}_1$ . Similar efficiency can be achieved to obtain samples of  $\boldsymbol{\theta}_2$  from  $p(\boldsymbol{\theta}_2 | \cdot) \equiv p(\boldsymbol{\theta}_2 | \mathbf{w}_2, \sigma_2^2)$ . That is, we seek the joint conditional distribution  $p(\boldsymbol{\theta}_2, \sigma_2^2 | \mathbf{w}_2)$ , and then integrate out  $\sigma_2^2$ .

### 3.2 Prediction for $Y(\mathbf{x}_0)$

For any design location  $\mathbf{x}_0 = (\mathbf{s}_0, \mathbf{u}_0) \in \mathcal{X}$ , our interest is to make prediction for  $Y(\mathbf{x}_0)$ , which is further written as

$$Y(\mathbf{x}_0) = \mathbf{h}(\mathbf{x}_0)^T \mathbf{b} + \mathbf{w}_1(\mathbf{x}_0) + \mathbf{w}_2(\mathbf{x}_0). \quad (3.8)$$

Define  $\Omega = \{\mathbf{b}, \sigma_1^2, \sigma_2^2, \tau^2, \boldsymbol{\theta}_1, \boldsymbol{\theta}_2\}$ . The (posterior) predictive distribution of  $Y(\mathbf{x}_0)$  given  $\mathbf{Z}$  is obtained as follows:

$$\begin{aligned} p(Y(\mathbf{x}_0) \mid \mathbf{Z}) &= \int p(Y(\mathbf{x}_0) \mid \mathbf{w}_1, \mathbf{w}_2, \Omega, \mathbf{Z}) \times p(\mathbf{w}_1, \mathbf{w}_2, \Omega \mid \mathbf{Z}) d\{\mathbf{w}_1, \mathbf{w}_2, \Omega\} \\ &= \int p(Y(\mathbf{x}_0) \mid \mathbf{w}_1, \mathbf{w}_2, \Omega) \times p(\mathbf{w}_1, \mathbf{w}_2, \Omega \mid \mathbf{Z}) d\{\mathbf{w}_1, \mathbf{w}_2, \Omega\}. \end{aligned} \quad (3.9)$$

Here, the distribution  $p(Y(\mathbf{x}_0) \mid \mathbf{w}_1, \mathbf{w}_2, \Omega)$  is the multivariate normal with mean  $\hat{Y}(\mathbf{x}_0) \equiv \mathbf{h}(\mathbf{x}_0)^T \mathbf{b} + \hat{\mathbf{w}}_1(\mathbf{x}_0) + \hat{\mathbf{w}}_2(\mathbf{x}_0)$ , and variance  $\hat{\sigma}^2(\mathbf{x}_0) = \hat{\sigma}_1^2(\mathbf{x}_0) + \hat{\sigma}_2^2(\mathbf{x}_0)$ , which are

$$\hat{\mathbf{w}}_1(\mathbf{x}_0) \equiv [\mathbf{R}_{nm} \mathbf{R}_*^{-1} \mathbf{R}(\mathbf{x}_0, \mathcal{X}^*)^T]^T \mathbf{R}_1^{-1} \mathbf{w}_1, \quad (3.10)$$

$$\hat{\mathbf{w}}_2(\mathbf{x}_0) \equiv (\rho_{1,0} \otimes \rho_{2,0})^T (\mathbf{R}_s \otimes \mathbf{R}_u)^{-1} \mathbf{w}_2, \quad (3.11)$$

$$\hat{\sigma}_1^2(\mathbf{x}_0) \equiv \sigma_1^2 - \sigma_1^2 [\mathbf{R}_{nm} \mathbf{R}_*^{-1} \mathbf{R}(\mathbf{x}_0, \mathcal{X}^*)^T]^T \mathbf{R}_1^{-1} \mathbf{R}_{nm} \mathbf{R}_*^{-1} \mathbf{R}(\mathbf{x}_0, \mathcal{X}^*)^T, \quad (3.12)$$

$$\hat{\sigma}_2^2(\mathbf{x}_0) \equiv \sigma_2^2 - \sigma_2^2 (\rho_{1,0} \otimes \rho_{2,0})^T (\mathbf{R}_s \otimes \mathbf{R}_u)^{-1} (\rho_{1,0} \otimes \rho_{2,0}), \quad (3.13)$$

with  $\rho_{1,0} \equiv (\rho_1(\mathbf{s}_0, \mathbf{s}_1), \dots, \rho_1(\mathbf{s}_0, \mathbf{s}_{n_1}))^T$  and  $\rho_{2,0} \equiv (\rho_2(\mathbf{u}_0, \mathbf{u}_1), \dots, \rho_2(\mathbf{u}_0, \mathbf{u}_{n_2}))^T$ .

Sampling from this predictive distribution involves inversion of matrices  $\mathbf{R}_1$  and  $\mathbf{R}_s \otimes \mathbf{R}_u$ , which can be done efficiently via the Sherman-Morrison-Woodbury formula in Eq. (A.4) and the property of Kronecker product of matrices in Eq. (A.4) in Appendix A. The resulting computational cost is  $O(m^3 + m^2 n + n_1^3 + n_2^3 + n(n_1 + n_2))$ . Samples from the predictive distribution  $p(Y(\mathbf{x}_0) \mid \mathbf{Z})$  can be obtained using composition sampling technique. That is, we draw from  $p(Y(\mathbf{x}_0) \mid \mathbf{w}_1, \mathbf{w}_2, \Omega)$ , with posterior samples of  $\mathbf{w}_1, \mathbf{w}_2, \Omega$  plugged into this distribution.

### 3.3 Alternative Specification for $w_1(\cdot)$

We describe AAGP and Bayesian inference of it using MPP to model  $w_1(\cdot)$ . An alternative computational-complexity-reduction method can be used for this component. For example, we can apply FSA to model  $w_1(\cdot)$ . The matrix  $\mathbf{V}$  in (2.4) will be replaced by a sparse matrix resulted from tapering in FSA. The proposed inference procedure described above can be applied efficiently. If MRA or NNGP is chosen to reduce computational complexity in  $w_1(\cdot)$ , the vector  $\mathbf{w}^*$  then will be high-dimensional, because these two methods using a smaller

number of conditioning set to construct a sparse precision matrix rather than resorting to a low-rank structure for the covariance matrix. The resulting covariance matrix  $\mathbf{R}_*^{-1}$  of  $\mathbf{w}^*$  is a sparse matrix. Therefore, our inference procedure can be implemented efficiently as well.

### 3.4 Missing Data Imputation

Recall that we represent  $\mathcal{X}$  as a product space  $\mathcal{X}_1 \times \mathcal{X}_2$  and have tentatively assumed that the response  $Z(\cdot)$  is observed at all  $n = n_1 n_2$  design locations, where  $n_1$  denotes the number of locations in  $\mathcal{X}_1$ , and  $n_2$  denotes that in  $\mathcal{X}_2$ . Now we relax this assumption and describe how missing data imputation can be carried out. Specifically, we introduce  $\mathcal{D}_c \equiv \{(\mathbf{s}_i, \mathbf{u}_j) : \mathbf{s}_i \in \mathcal{X}_1, \mathbf{u}_j \in \mathcal{X}_2, i = 1, \dots, n_1; j = 1, \dots, n_2\}$  to denote the complete grid over  $\mathcal{X} = \mathcal{X}_1 \times \mathcal{X}_2$ . We assume that the response variable  $Z(\cdot)$  is only observed at a subset of  $n$  ( $n < n_1 n_2$ ) design locations  $\mathcal{D}_o \equiv \{\mathbf{x}_1, \dots, \mathbf{x}_n\} \subset \mathcal{D}_c$ . The resulting  $n$ -dimensional data vector is denoted by  $\mathbf{Z}_o$ , and we let  $\mathbf{Z}_m$  denote the  $(n_1 n_2 - n)$ -dimensional vector of  $Z(\cdot)$  at the unobserved design locations in  $\mathcal{D}_m \equiv \mathcal{D}_c \setminus \mathcal{D}_o$ . In the Metropolis-within-Gibbs sampler, we now use  $\mathbf{w}_1$ ,  $\mathbf{w}_2$ , and  $\mathbf{Z}$  to represent the  $(n_1 n_2)$ -dimensional vectors at all design locations in  $\mathcal{D}_o$ , and treat  $\mathbf{Z}_m$  as unknown. The full conditional distributions and sampling procedure for parameters  $\{\mathbf{b}, \tau^2, \sigma_1^2, \sigma_2^2, \boldsymbol{\theta}_1, \theta_2\}$  and random effects  $\mathbf{w}^*$ ,  $\mathbf{w}_1$  and  $\mathbf{w}_2$  are the same as described in Section 3.1. The missing values  $\mathbf{Z}_m$  can also be easily updated in MCMC based on its full conditional distribution. Actually, it can be shown that  $[\mathbf{Z}_m \mid \cdot] = \mathcal{N}(\mathbf{Y}_m, \tau^2 \mathbf{I})$ , where  $\mathbf{Y}_m \equiv \mathbf{H}_m \mathbf{b} + \mathbf{w}_{1,m} + \mathbf{w}_{2,m}$ , and  $\mathbf{H}_m$ ,  $\mathbf{w}_{1,m}$ , and  $\mathbf{w}_{2,m}$  denote the matrix of covariates and subsets of the random effects  $\mathbf{w}_1$  and  $\mathbf{w}_2$  over the unobserved locations in  $\mathcal{D}_m$ , respectively.

## 4 Numerical Illustrations

This section presents several simulation examples under different scenarios to illustrate the model accuracy and prediction accuracy. The proposed method additive approximate Gaussian process is compared with modified predictive process and full Gaussian process, where the full Gaussian process is referred to as full GP, and is used as benchmark in the

synthetic examples. The proposed method is also applied to analyze Eastern US ozone data. All the methods are implemented in MATLAB R2015b, and the algorithms are run in a 10-core HP Intel Xeon E5-2680 machine with 12 GB random-access memory.

## 4.1 Motivating Example: Two-Dimensional Input Space

To see how accurate is the approximation of MPP and AAGP to emulate a deterministic function, we consider the function  $f(x_1, x_2) = 10x_1 \exp(-\sqrt{x_1^2 + x_2^2})$ , where the input  $\mathbf{x} = (x_1, x_2) \in \mathcal{X} = [-6, 6] \times [-6, 6]$ . We first simulated data with the function  $f(\cdot, \cdot)$  evaluated at  $n = 50 \times 50$  regular grids in the domain. Then we randomly held out 10% for prediction. The remaining 90% of data are used for parameter estimation. We compared four methods: 1) full GP with Gneiting's nonseparable correlation function; 2) full GP with Gneiting's nonseparable correlation function and separable correlation function with exponential correlation functions for the first and second dimension; 3) MPP with Gneiting's nonseparable correlation function; 4) AAGP with Gneiting's nonseparable correlation function and separable correlation function with exponential correlation functions for the first and second dimension. 80 knots are selected in the domain via nested hyperlatin cube design. The MCMC for these four GP models are run 25,000 iterations with a burn-in 15,000 iterations. All the posterior samples converged from our exploratory analysis. The results are reported in Table 1. We can see that the MSPE for full GP with two component are smallest. The MSPE for full GP with one components and AAGP are similar, and close to the results. The results from MPP has largest MSPE among all the methods. The computational time in AAGP is roughly twice as the time in MPP, and is only 7% of the time in full GP with two components, and 11% of time in full GP with just one component. The use of AAGP clearly shows its inferential benefit over MPP and computational advantage over full GP.

**Table 1.** Simulation results with a deterministic function.

	Full GP (one component)	Full GP (two components)	MPP	AAGP
MSPE	$1.31 \times 10^{-4}$	$7.60 \times 10^{-5}$	$2.22 \times 10^{-2}$	$1.19 \times 10^{-4}$
Time (h)	14.5	22.3	0.81	1.70

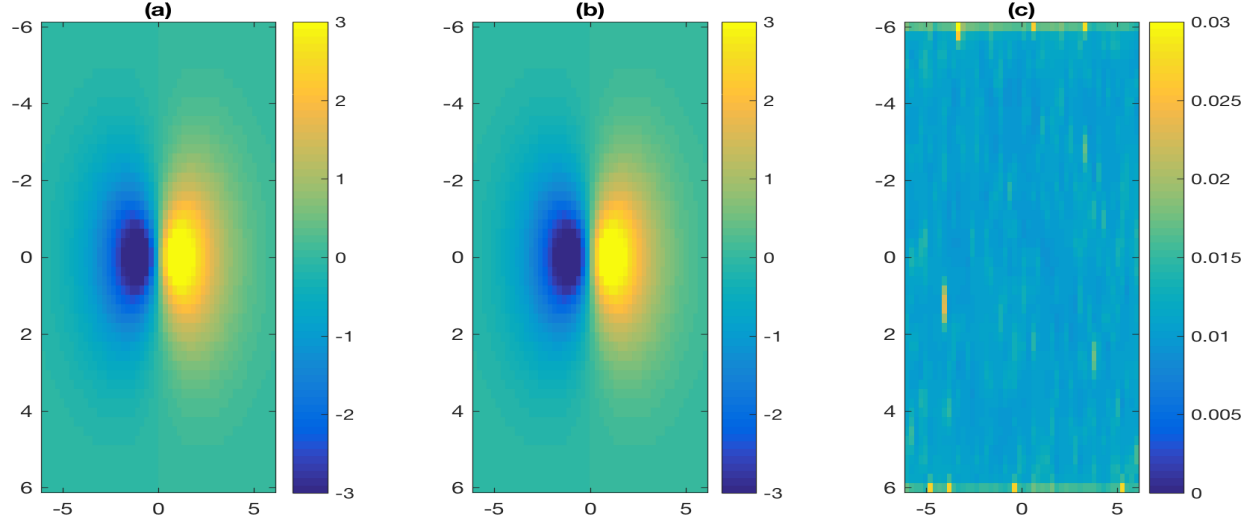


**Figure 1.** Results for deterministic function. Panel (a) shows the deterministic function evaluated at  $50 \times 50$  grids. Panel (b) shows the posterior mean from AAGP based on 90% randomly selected datasets. Panel (c) shows the posterior standard errors of the predictions over all 50-by-50 grids from AAGP.

## 4.2 Artificial Examples: Three-Dimensional Input Space

To demonstrate the computational and prediction advantage our proposed method, three different scenarios with different covariance function structures are considered for simulated true field  $Y(\cdot)$  in a spatio-temporal domain  $\mathcal{X} \equiv [0, 20]^2 \times [1, 20]$ . Specifically, we consider the following three scenarios: 1) Gneiting's space-time nonseparable correlation function only (First Scenario); 2) separable covariance function only for (Second Scenario); and 3) Gneiting's space-time nonseparable correlation function and separable covariance function for (Third Scenario). The covariates in trend term contain  $h_1(\mathbf{x}), h_2(\mathbf{x})$ , where  $h_1(\mathbf{x})$  is simulated for standard normal distribution, and  $h_2(\mathbf{x}) = \cos(\mathbf{1}^T \mathbf{x})$  for  $\mathbf{x} \in \mathcal{X}$ . The true process  $Y(\cdot)$  is simulated on 225 randomly selected spatial locations in two dimensional space  $\mathcal{X}_1 \equiv [0, 20] \times [1, 20]$  and 20 locations in time  $\mathcal{X}_2 \equiv [1, 20]$ , which results in 4500 locations in the spatio-temporal domain  $\mathcal{X}$ . The data are obtained by adding measurement noise or nugget effect. For all the simulated data, 90% of them are randomly selected as training set to carry out Bayesian inference, and the remaining 10% are used to compare the predictive performance.

In each scenario, three different model inference have been applied: (a) full GP, (b) MPP

and (c) the proposed AAGP. The full Gaussian process based on true covariance function is used to serve as a benchmark. For each model, independent prior distributions are assigned for all their parameters. In specific, the prior distribution for the mean components are specified as  $\mathbf{b} \sim \mathcal{N}_2(\mathbf{0}, 1000\mathbf{I})$ . The prior distributions for the parameters in Gneiting's space-time correlation function are assigned as  $\sigma_1^2 \sim \mathcal{IG}(2, 0.01)$ ,  $a \sim U(0, 20)$ ,  $c \sim U(0, 100)$ ,  $\beta \sim U(0, 1)$ . For the variance of the nugget, we assign  $\tau^2 \sim \mathcal{IG}(2, 0.01)$  prior distribution. For the AAGP and full GP, when needed, we also specify prior distributions for the separable space-time covariance function as  $\sigma_2^2 \sim \mathcal{IG}(2, 0.01)$ ,  $\phi_s \sim U(0, 100)$ ,  $\phi_t \sim U(0, 20)$ . The smoothness parameter  $\alpha$  is fixed at 0.5. The MCMC algorithm is run 25000 iterations for full GP, MPP and AAGP. The results are based on last 15000 of MCMC samples. The computational time is recorded based on the total time for 25000 MCMC iterations. For MPP and AAGP, 25 knots in space and 10 knots in time are uniformly selected in the spatio-temporal domain. In addition, we also add very small fixed nuggets to spatial and temporal separable correlation matrices  $\mathbf{R}_s$  and  $\mathbf{R}_u$  to avoid numerical instabilities in MCMC algorithm, since their inverses are required. As tools of comparison, for all three scenarios, we use: posterior summary for 50 (2.5, 97.5) percentiles of model parameters, mean-squared-prediction error (MSPE), and average length of 95% credible intervals (ALCI) for predictive values, to assess model adequacy and predictive accuracy.

**First Scenario** The latent true process  $Y(\cdot)$  is assumed to have a Gneiting's space-time covariance function in Eq. (B.1) with variance  $\sigma_1^2 = 1$ , spatial parameter  $c = 5$ , time parameter  $a = 1$ , nugget variance  $\tau^2 = 0.2$ , interaction parameter  $\beta = 0.8$ , and smoothness parameter  $\alpha = 0.5$ . The linear components are  $\mathbf{b} = (1, 0.5)^T$ . We compare the results of AAGP with the space-time MPP and the full Gaussian process. The full Gaussian process based on true covariance function is used to serve as a benchmark. The prior distributions are assigned as described above.

Table 2 shows the results obtained from three different methods. The true values for parameters  $\mathbf{b}, \sigma_1^2, \beta, a, c, \sigma_2^2, \phi_s, \phi_t, \tau^2$  are listed in the second column of table 2. AAGP gives better prediction results than MPP, since the MSPE in AAGP is 30% smaller than that in MPP, and is close to MSPE in the full GP. This confirms that the separable component of the AAGP can model part of the unexplained variability from the MPP. The spread

**Table 2.** Simulation results under Gneiting’s space-time correlation function

Parameters	True value	First Scenario		
		Full GP	MPP	AAGP
$b_1$	1	0.989(0.980, 0.998)	0.990(0.981, 1.000)	0.981(0.959, 1.007)
$b_2$	0.5	0.503(0.473, 0.533)	0.503(0.491, 0.516)	0.507(0.468, 0.534)
$\sigma_1^2$	1	0.978(0.869, 1.096)	1.419(1.236, 1.645)	0.869(0.787, 1.038)
$\beta$	0.8	0.841(0.425, 0.994)	0.935(0.710, 0.999)	0.928(0.631, 0.997)
$a$	1	0.991(0.754, 1.255)	2.070(1.613, 2.659)	2.805(2.054, 3.872)
$c$	5	4.768(4.022, 5.710)	5.465(4.503, 6.560)	5.542(4.685, 6.750)
$\sigma_2^2$				0.303(0.221, 0.341)
$\phi_s$				0.244(0.035, 0.488)
$\phi_t$				1.370(1.344, 1.417)
$\tau^2$	0.2	0.182(0.146, 0.221)	0.130(0.049, 0.208)	0.060(0.021, 0.130)
MSPE		0.23	0.51	0.33
ALCI		1.92	3.24	2.97
Time (h)		21.2	3.94	5.01

of predictive distribution is very similar for both MPP and AAGP, which suggests that MPP and AAGP can quantify uncertainties in predictions very well, but the predictive distribution for AAGP is slightly accurate than that for MPP. In AAGP, the regression coefficients  $b_1, b_2$  are estimated very well in comparison to the full GP results. The mean of the posterior for the variance parameters  $\sigma_1^2 = 0.869$  and  $\sigma_2^2 = 0.303$ . The AAGP shows a clear preference for the Gneiting’s nonseparable covariance function in this case. The proposed model seems to be able to automatically assign the variation missed by MPP to the separable model and the nugget. Despite the fact that the nugget is under-estimated and the overall variance  $\sigma_1^2 + \sigma_2^2$  overestimated, the prediction performance of the proposed method is better. One possible explanation of the above value is that the sum of estimated  $\sigma_2^2$  and  $\tau^2$  both together plays a role as “nugget effect”. It is worth noting that the space-time interaction parameter  $\beta$  has very wide credible interval in full GP, which indicates that this parameter cannot be estimated accurately even under the true model.

**Second Scenario** The latent true process  $Y(\cdot)$  is assumed to have a squared exponential covariance functions in space and time with variance  $\sigma_2^2 = 1$ , spatial correlation parameter  $\phi_s = 5$ , time correlation parameter  $\phi_t = 1$ , and nugget variance  $\tau^2 = 0.2$ . The linear components are defined as  $\mathbf{b} = (1, 0.5)^T$ . As previously, we compare AAGP and the space-time MPP and use the full GP based on true covariance function as a benchmark. In

the MPP, the parent correlation function is assumed to be Gneiting's space-time correlation function. The prior distributions are specified as above.

**Table 3.** Simulation results under separable correlation function

Parameters	True value	Second Scenario		
		Full GP	MPP	AAGP
$b_1$	1	0.989(0.975, 1.004)	1.003(0.973, 1.033)	0.989(0.974, 1.003)
$b_2$	0.5	0.503(0.483, 0.522)	0.498(0.455, 0.542)	0.503(0.484, 0.522)
$\sigma_1^2$			0.083(0.045, 0.163)	0.030(0.012, 0.060)
$\beta$			0.737(0.104, 0.987)	0.554(0.027, 0.982)
$a$			0.768(0.378, 1.564)	9.425(2.390, 20.00)
$c$			17.81(9.540, 20.00)	0.198(0.023, 0.835)
$\sigma_2^2$	1	0.953(0.752, 1.195)		0.997(0.830, 1.187)
$\phi_s$	5	4.968(4.646, 5.213)		5.169(4.922, 5.262)
$\phi_t$	1	0.990(0.918, 1.067)		1.005(0.940, 1.083)
$\tau^2$	0.2	0.188(0.179, 0.196)	0.950(0.992, 1.037)	0.187(0.178, 0.196)
MSPE		0.02	0.87	0.02
ALCI		0.58	0.98	0.69
Time (h)		40.9	1.39	2.78

Simulation results in Table 3 suggest that MPP fails to detect the separability of the true field with Gneiting's space-time correlation function, since  $\beta$  has 95% credible interval spreading out almost its entire support  $[0, 1]$ . Compared to MPP, AAGP can detect the separability and has much better prediction results. The variance parameter  $\sigma_1^2$  is close to 0, and variance parameter  $\sigma_2^2$  is close to 1, which indicates that the AAGP is able to select the most appropriate model for the data. The prediction results in AAGP are very close to the results of the full GP, and much better than that obtained from MPP. The trend parameters  $b_1, b_2$  can also be estimated very well. It can be seen that the posterior mean of the variance parameters  $\sigma_1^2$  and  $\sigma_2^2$ , which serve as weights for the two components, are correctly identified:  $\sigma_1^2 = 0.03$  and  $\sigma_2^2 = 0.996$ . The results in MPP also show that disadvantage is obvious when MPP is used to approximate the covariance function that is not the same one implied by the data, as the estimate of nugget is even larger than the estimate of variance in MPP. The failure of MPP on detecting correctly the separability may also rely on the fact the Gneiting's space-time correlation function is not as smooth as the process with squared exponential correlation function. To improve results for MPP, we tried to let  $\alpha$  in a range of values. However, this leads to computational instabilities in

the MCMC.

**Third Scenario** The last simulation example addresses the problem of parameter estimation and predictive performance in AAGP under true covariance function model. The process  $Y(\cdot)$  is simulated from an additive Gaussian process with Gneiting's space-time covariance and a separable squared exponential covariance function. The parameters in the Gneiting's space-time covariance function component have variance  $\sigma_1^2 = 1$ , spatial parameter  $c = 5$ , temporal parameter  $a = 1$ , interaction parameter  $\beta = 0.8$ , and smoothness parameter  $\alpha = 0.5$ . The parameters of the separable space and time component have variance  $\sigma_2^2 = 1$ , spatial correlation parameter  $\phi_s = 5$ , time correlation parameter  $\phi_t = 1$ . The linear components are  $\mathbf{b} = (1, 0.5)^T$ , and the nugget variance is  $\tau^2 = 0.2$ .

The results of this example are given in Table 4. Compared to MPP, the MSPE in AAGP is 66% smaller than that in MPP, and close to the MSPE in full GP. The predictive performance in AAGP is relatively close to the predictive performance of the full GP. The posterior mean of  $b_1, b_2, \beta, \sigma_2^2, \phi_s, \phi_t$  are well estimated in AAGP. The variance parameter  $\sigma_1^2$  and range parameters  $a$  are slightly over-estimated. We also observe that the nugget is underestimated in AAGP. This is likely because there are fixed small constants  $\tau_s^2, \tau_u^2$  are added to the diagonal of the separable correlation matrices  $\mathbf{R}_s$  and  $\mathbf{R}_u$ , and it makes the nugget term to be  $(\tau^2 + \tau_s^2 \tau_u^2) \mathbf{I}_n$  instead of  $\tau^2 \mathbf{I}_n$ . As the variance parameters  $\sigma_1^2$  and  $\sigma_2^2$  are correctly identified in AAGP, the proposed model AAGP is able to correctly identify the variation coming from the non-separable and separable part. The range parameter  $c$  in AAGP is over-estimated, and this is likely due to the overestimation of the variance parameter  $\sigma_1^2$ , since their ratio plays an important role in predictions under certain conditions (Kaufman and Shaby, 2013).

**Summary** In all the examples above AAGP has better prediction performance than MPP, regardless of the simulation settings. This is even true for scenario 1 where the covariance function favor the MPP. Moreover, AAGP seems to be more robust than MPP when the covariance function is misspecified. MPP has poor predictive performance if the covariance function is misspecified; see the results in Table 3 and Table 4. Instead, the predictive performance of AAGP is close to the predictive performance of the full GP, see the results in Table 2 and Table 3. The AAGP seems to give more accurate results under

**Table 4.** Simulation results under a combination of nonseparable and separable correlation functions

Parameters	True value	Third Scenario		
		Full GP	MPP	AAGP
$b_1$	1	0.995(0.944, 0.999)	0.969(0.932, 1.007)	0.969(0.949, 0.997)
$b_2$	0.5	0.502(0.472, 0.532)	0.499(0.446, 0.552)	0.509(0.475, 0.540)
$\sigma_1^2$	1	0.993(0.863, 1.204)	1.615(1.319, 1.957)	1.356(1.181, 1.463)
$\beta$	0.8	0.847(0.396, 0.994)	0.897(0.539, 0.996)	0.848(0.332, 0.993)
$a$	1	0.961(0.705, 1.316)	2.379(1.324, 3.677)	1.737(1.409, 2.248)
$c$	5	4.758(3.857, 6.226)	4.973(3.660, 6.639)	8.253(6.711, 10.43)
$\sigma_2^2$	1	0.916(0.730, 1.172)		0.970(0.806, 1.154)
$\phi_s$	5	4.889(4.529, 5.213)		5.047(4.878, 5.150)
$\phi_t$	1	1.003(0.926, 1.071)		1.037(0.989, 1.095)
$\tau^2$	0.2	0.175(0.141, 0.211)	0.583(0.236, 0.795)	0.056(0.019, 0.155)
MSPE		0.28	1.40	0.48
ALCI		2.10	3.85	3.40
Time (h)		106	1.44	3.47

misspecified covariance function model, and this is especially important when statistical models are used to analyze real spatial and spatio-temporal datasets with unknown covariance structures. We also noticed that the AAGP that incorporates covariance function from MPP does not provide an exact approximation for the true covariance function. Although the discrepancy between the true covariance function and the covariance function resulting from AAGP cannot be eliminated, the second component in AAGP can greatly improve the prediction results. In addition, the AAGP can provide a computational strategy to make fast Bayesian inference when existing methods such as computational-complexity-reduced methods or separable covariance function are combined to improve inferential results. We can further improve the results of AAGP, if we select the knots of the MPP in a more sophisticated way (Guhaniyogi et al., 2011; Zhang et al., 2015b). However, this is out of the scope of this paper.

The computing time for AAGP is roughly twice as the computing time for MPP. The AAGP is much faster than the full GP. It is worth mentioning that the computational time to construct covariance matrix is slow but unavoidable. The computational time to construct full GP in Table 4 is much larger than either the computational time in Table 2 or the computational time in Table 3, since constructing two correlation matrices  $\mathbf{R}_0, \mathbf{R}_2$  takes more time than just constructing one correlation matrix  $\mathbf{R}_1$  or  $\mathbf{R}_2$ . In addition,

constructing the correlation matrices  $\mathbf{R}_1, \mathbf{R}_*$  five times takes about 30% of the time in one MCMC iteration in MPP, since these matrices need to be evaluated five times in one MCMC iteration. This unavoidable time can make the MPP as well as AAGP slow when the high-dimensional input domain is under study.

### 4.3 Analysis of Eastern US Ozone Data

Ground-level ozone ( $\text{O}_3$ ) is one of six common air pollutants identified in the Clean Air Act, and these air pollutants are called “criteria pollutants” by the U.S. Environmental Protection Agency (EPA). To protect human health and the environment, EPA publishes the National Ambient Air Quality Standards (NAAQS) for ozone, which specifies the maximum allowed measurement for ozone to be present in the outdoor air. The NAAQS for ozone is calculated based on the following steps: 1) the maximum 8-hour average is calculated for each day; 2) then the fourth-highest value is computed for these daily maximum 8-hour averages; 3) finally, the NAAQS for ozone is defined as the average of these fourth-highest values for any consecutive three-year period. The proposed method is illustrated with daily maximum 8-hour average data at a network of monitoring sites in the eastern U.S. from April through October in the year 1995 to 1999. This data has been widely used in environmental statistics (see, for example, Fuentes, 2003; Gilleland and Nychka, 2005; Zhang et al., 2015b), and can be obtained on the website at <https://www.image.ucar.edu/Data/Ozmax>. Following the pre-processing steps in Gilleland and Nychka (2005), the daily maximum 8-hour ozone average at station  $\mathbf{s}$  and day  $t$ , denoted by  $O(\mathbf{s}, t)$ , is assumed to have the following structure  $O(\mathbf{s}, t) = \mu(\mathbf{s}, t) + \tilde{O}(\mathbf{s}, t)$ , where  $\mu(\mathbf{s}, t) = a(\mathbf{s}) + \sum_{j=1}^3 \{b_j \cos(2\pi jt/184) + c_j \sin(2\pi jt/184)\}$ , which models the seasonal effect. The coefficients in the seasonal effect  $\mu(\mathbf{s}, t)$  are estimated through ordinary least square method. The spatial-varying standard deviation  $k(\cdot)$  is estimated with the empirical standard deviation based on residuals after removing the seasonal effect. The residual  $r(\mathbf{s}, t) \equiv O(\mathbf{s}, t) - \hat{\mu}(\mathbf{s}, t)$  scaled by its estimated standard deviation  $\hat{k}(\cdot)$  at each station is referred to as *standardized ozone* at station  $\mathbf{s}$  and time  $t$  hereafter. The spatio-temporal model (2.1) with zero mean is assumed for the standardized ozone, based upon which statistical inference is carried out.

The datasets used in this paper are obtained at 513 monitoring sites during 92 days from June to August in 1997, where  $1.37\% = 645/(513 \times 92) \times 100\%$  of data are missing, and only 46551 data points are observed. In what follows, statistical analysis is carried out on the standardized data using the previously mentioned pre-processing steps. To analyze these data, a cross-validation is first carried out on observed 46551 data points on June to August in 1997, where 90% randomly selected data points are used for parameter estimation, and the remaining 10% data points are used to assess predictive performance. In the cross-validation, two covariance function models are compared: the MPP with Gneiting's space-time covariance function as parent covariance function, and the AAGP with Gneiting's space-time covariance function and exponential covariance functions in the separable covariance function. The prior distributions are specified as  $\sigma_1^2 \sim \mathcal{IG}(2, 0.01)$ ,  $\sigma_2^2 \sim \mathcal{IG}(2, 0.01)$ ,  $\tau^2 \sim \mathcal{IG}(2, 0.01)$ ,  $a \sim U(0, 60)$ ,  $c \sim U(0, 2000)$ ,  $\beta \sim U(0, 1)$  in Gneiting's space-time correlation function and  $\phi_s \sim U(0, 2000)$ ,  $\phi_t \sim U(0, 60)$  in separable covariance functions in space and time. In MPP and AAGP, 490 knots are selected in the spatio-temporal domain via hyperlatin design. The distance in space is calculated based on chordal distance, and the distance in time is calculated based on Euclidean distance.

For the cross-validation, the results in Table 5 show that AAGP gives better predictive performance than MPP. The variance for Gneiting's nonseparable covariance function in MPP is much larger than the variance estimated in AAGP, but the overall variance is estimated consistently based on MPP and AAGP. There two spatial range parameters  $c, \phi_s$  and two temporal range parameters  $a, \phi_t$  in AAGP. The meaning of these parameters should not be confused with corresponding parameters in the covariance function model with just only one of the components. Although the time in AAGP is longer than MPP (roughly a factor of 2.3), the improved prediction accuracy is noticeable.

What follows is to carry out predictions based on all observed data in the entire Eastern US region. Figure 2 shows the predictions on three consecutive days based on all available data, which clearly shows that AAGP is able to capture the spatial-temporal dependence structures in the data.

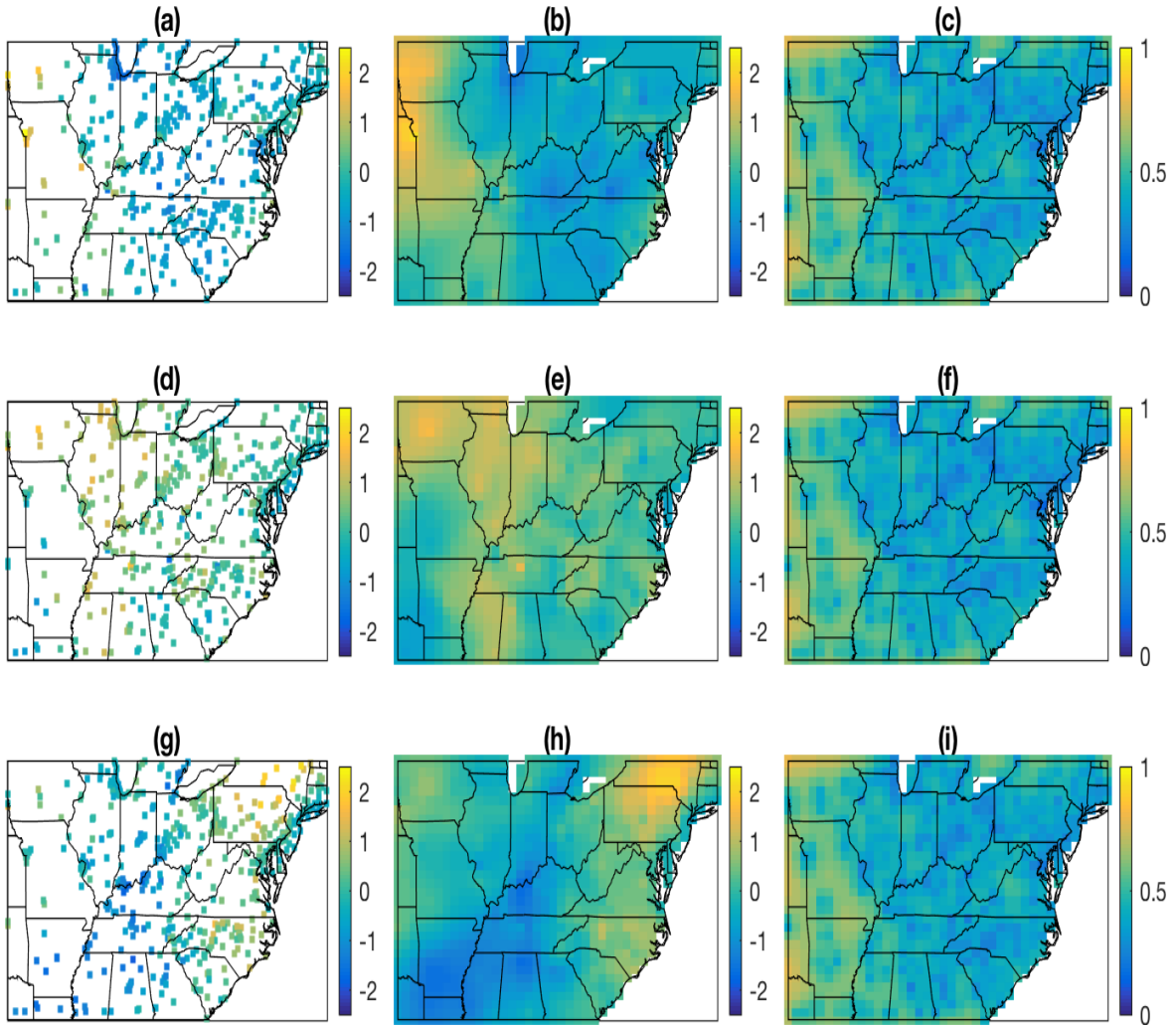


**Figure 2.** Standardized ozone data and predictions for  $Y(\cdot)$  based on 30 by 40 locations on three consecutive days (unit: parts per million). The panels (a), (d), (g) show the standardized ozone on June 14, 15, 16 in 1997. The panels (b), (e), (h) show the posterior mean on June 14, 15, 16 in 1997. The panels (c), (f), (i) shows the corresponding posterior standard errors.

**Table 5.** Cross validation results for standardized ozone from June to August, 1997. Gneiting's nonseparable correlation function is used in full GP and MPP. Exponential correlation functions are used for separable covariance function in AAGP.

Parameters	MPP	AAGP
$\sigma_1^2$	0.8530(0.796, 0.914)	0.097(0.085, 0.137)
$\beta$	0.973(0.996, 1.000)	0.017(0, 0.101)
$a$ (day)	1.674(1.557, 1.782)	5.196(3.932, 7.112)
$c$ (km)	1508(1406, 1625)	1999(1996, 2000)
$\sigma_2^2$		0.806(0.756, 0.870)
$\phi_s$ (km)		280.1(261.8, 302.9)
$\phi_t$ (day)		1.85(1.78, 1.93)
$\tau^2$	0.194(0.187, 0.202)	0.041(0.035, 0.044)
MSPE	0.41	0.13
ALCI	1.88	1.05
Time (h)	41.8	87.7

## 5 Conclusion and Discussion

In this paper, we have proposed a new Gaussian process approximation scheme based on two separate additive computationally efficient components: a) a modified predictive process, and b) a separable covariance function. The resulting covariance function in additive approximate Gaussian process is nonseparable and allows data to determine how much variation is explained by these two components, and thus provides a flexible way to characterize spatial dependence structure. As shown in the paper, the new covariance function does not inherit the same computational flexibility as its separate components. To overpass this computational challenges we have proposed a fully conditional Markov chain Monte Carlo algorithm, based on the hierarchical model representation. Moreover, we introduced numerical stability in the covariance function by adding a nugget term without increasing the computational complexity of the model. The AAGP is introduced in a general context, and is applied in a spatio-temporal setting. This can be extended to build surrogate models in applications with expensive computer models, where the input dimension can be large. Computational advantage is inherited based on the computational-complexity-reduced method and a separable covariance function. When modeling separability for high dimensional input domain, domain knowledge will help decide which part of inputs do not interact with other part of inputs. To access the performance of the proposed approxima-

tion method, we have applied and compare its performance in four different simulations examples under different settings. We have also applied the proposed AAGP to the eastern US ozone spatio-temporal data set. In all these cases the improvement in the prediction are significant and the computational cost is relatively low.

Alternative computational-complexity-reduction methods can be used for both component in the AAGP framework. For example, we can apply FSA to model the first component and separable covariance to model the second component. One can also use MRA or NNGP to reduce computational complexity as well. The fully conditional MCMC algorithm can be extended to enables fast posterior sampling and predictions with large datasets when a covariance function admits a more general additive form of multiple components. However, a more rigorous algorithmic development as well as comparison fave been left for future work. Also when the dimensions of separable covariance matrices are large, i.e.,  $n_1$  or  $n_2$  is large, our method can be generalized. For example, a computational-complexity-reduction method can be embedded to approximate  $\mathbf{R}_s$  or  $\mathbf{R}_u$ , correspondingly. Moreover, efficiency of the proposed Bayesian inference procedure can be improved using partially collapsed Gibbs samplers (van Dyk and Park, 2008; van Dyk and Jiao, 2015).

## Acknowledgement

This work was supported in part by an allocation of computing time from the Ohio Supercomputer Center. Ma's research was supported by the Charles Phelps Taft Dissertation Fellowship at the University of Cincinnati. Kang's research was partially supported by the Simons Foundation's Collaboration Award (NO. 317298) and the Taft Research Center at the University of Cincinnati.

# Appendix

## A Technical details

**Fact 1** (Properties related to Kronecker product). *For any symmetric positive definite  $n_1$ -by- $n_1$  matrix  $\mathbf{R}_s$  and  $n_2$ -by- $n_2$  matrix  $\mathbf{R}_u$ , the following matrix identities hold,*

$$\mathbf{R}_s \otimes \mathbf{R}_u = (\mathbf{L}_1 \otimes \mathbf{L}_2)(\mathbf{L}_1 \otimes \mathbf{L}_2)^T \quad (\text{A.1})$$

$$\mathbf{R}_s \otimes \mathbf{R}_u = (\mathbf{U}_1 \otimes \mathbf{U}_2)(\mathbf{\Lambda}_1 \otimes \mathbf{\Lambda}_2)(\mathbf{U}_1 \otimes \mathbf{U}_2)^T \quad (\text{A.2})$$

$$\text{vec}(\mathbf{T}) = (\mathbf{R}_s \otimes \mathbf{R}_u)\text{vec}(\mathbf{K}) \iff \mathbf{T} = \mathbf{R}_u \mathbf{K} \mathbf{R}_s^T, \quad (\text{A.3})$$

$$\text{vec}(\mathbf{T}) = (\mathbf{R}_s \otimes \mathbf{R}_u)^{-1}\text{vec}(\mathbf{K}) \iff \mathbf{T} = \mathbf{R}_u^{-1} \mathbf{K} \mathbf{R}_s^{-T}, \quad (\text{A.4})$$

$$|\mathbf{R}_s \otimes \mathbf{R}_u| = |\mathbf{R}_s|^{n_2} |\mathbf{R}_u|^{n_1}, \quad (\text{A.5})$$

$$[(\sigma_2^2 \mathbf{R}_s \otimes \mathbf{R}_u)^{-1} + (\tau^2 \mathbf{I})^{-1}]^{-1} = (\mathbf{U}_1 \otimes \mathbf{U}_2) \left( \frac{1}{\sigma_2^2} \mathbf{\Lambda}_1^{-1} \otimes \mathbf{\Lambda}_2^{-1} + \frac{1}{\tau^2} \mathbf{I} \right)^{-1} (\mathbf{U}_1 \otimes \mathbf{U}_2)^T, \quad (\text{A.6})$$

where  $\mathbf{R}_s = \mathbf{L}_1 \mathbf{L}_1^T$  is the Cholesky decomposition for  $\mathbf{R}_s$ , and  $\mathbf{R}_s = \mathbf{U}_1 \mathbf{\Lambda}_1 \mathbf{U}_1^T$  is the eigenvalue decomposition of  $\mathbf{R}_s$ , and similarly for  $\mathbf{R}_u$ .

**Remark 1.** The computational cost is reduced from  $O(n^2)$  to  $O(n(n_1 + n_2))$  in (A.3), from  $O(n^3/3)$  to  $O(n(n_1 + n_2) + n_1^3/3 + n_2^3/3)$  in (A.4), from  $O(n^3/3)$  to  $O(n_1^3/3 + n_2^3/3)$  in (A.5).

**Fact 2.** Given  $m$ -by- $m$  positive definite matrix  $\mathbf{R}_*$ ,  $n$ -by- $m$  full column rank matrix  $\mathbf{R}_{nm}$ , and diagonal matrix  $\mathbf{V}$ , the following equation holds for  $\mathbf{R}_1 \equiv \mathbf{V} + \mathbf{R}_{nm} \mathbf{R}_*^{-1} \mathbf{R}_{nm}^T$ ,

$$\mathbf{R}_1^{-1} = \mathbf{V}^{-1} - \mathbf{V}^{-1} \mathbf{R}_{nm} (\mathbf{R}_* + \mathbf{R}_{nm}^T \mathbf{V}^{-1} \mathbf{R}_{nm})^{-1} \mathbf{R}_{nm}^T \mathbf{V}^{-1} \quad (\text{A.7})$$

**Remark 2.** The inversion of  $\mathbf{R}_1$  requires computational cost  $O(nm^2)$ .

## B Correlation Functions

The Gneiting's nonseparable correlation function is

$$\rho((\mathbf{s}, t), (\mathbf{s}', t')) = \left( \frac{|t - t'|^{2\alpha}}{a} + 1 \right)^{-d/2} \exp \left\{ -\frac{\|\mathbf{s} - \mathbf{s}'\|}{c \left( \frac{|t - t'|^{2\alpha}}{a} + 1 \right)^{\beta/2}} \right\}, \quad (\text{B.1})$$

where  $d$  is the dimension of space;  $a$  is range parameter in time;  $c$  is the range parameter in space;  $\alpha \in (0, 1]$  is the smoothness parameter of the temporal part;  $\beta \in [0, 1]$  is the space-time interaction parameter.

The squared exponential correlation function is

$$\rho(d) = \exp\left(-\frac{d^2}{2\phi^2}\right), \quad (\text{B.2})$$

where  $d$  is the distance in space or time, and  $\phi$  is the range parameter in space or time.

The exponential covariance function is

$$\rho(d) = \exp\left(-\frac{d}{\phi}\right), \quad (\text{B.3})$$

where  $d$  is the distance in space or time, and  $\phi$  is the range parameter in space or time.

## References

Ba, S. and Joseph, V. R. (2012). Composite Gaussian process models for emulating expensive functions. *The Annals of Applied Statistics*, 6(4):1838–1860.

Banerjee, S., Carlin, B. P., and Gelfand, A. E. (2014). *Hierarchical Modeling and Analysis for Spatial Data, Second Edition*. CRC Press.

Banerjee, S., Gelfand, A. E., Finley, A. O., and Sang, H. (2008). Gaussian predictive process models for large spatial data sets. *Journal of the Royal Statistical Society: Series B (Statistical Methodology)*, 70(4):825–848.

Bilionis, I., Zabaras, N., Konomi, B. A., and Lin, G. (2013). Multi-output separable gaussian process: Towards an efficient, fully bayesian paradigm for uncertainty quantification. *Journal of Computational Physics*, 241:212–239.

Conti, S. and O'Hagan, A. (2010). Bayesian emulation of complex multi-output and dynamic computer models. *Journal of Statistical Planning and Inference*, 140(3):640–651.

Cressie, N. (1993). *Statistics for Spatial Data*. John Wiley & Sons, New York, revised edition.

Cressie, N. and Johannesson, G. (2008). Fixed rank kriging for very large spatial data sets. *Journal of the Royal Statistical Society: Series B (Statistical Methodology)*, 70(1):209–226.

Cressie, N. and Wikle, C. K. (2011). *Statistics for Spatio-Temporal Data*. John Wiley & Sons, New York.

Curran, C., Mitchell, T., Morris, M., and Ylvisaker, D. (1991). Bayesian prediction of deterministic functions, with applications to the design and analysis of computer experiments. *Journal of the American Statistical Association*, 86(416):953–963.

Datta, A., Banerjee, S., Finley, A. O., and Gelfand, A. E. (2016a). Hierarchical nearest-neighbor Gaussian process models for large geostatistical datasets. *Journal of the American Statistical Association*, 111(514):800–812.

Datta, A., Banerjee, S., Finley, A. O., Hamm, N. A. S., and Schaap, M. (2016b). Nonseparable dynamic nearest neighbor Gaussian process models for large spatio-temporal data with an application to particulate matter analysis. *The Annals of Applied Statistics*, 10(3):1286–1316.

Finley, A. O., Sang, H., Banerjee, S., and Gelfand, A. E. (2009). Improving the performance of predictive process modeling for large datasets . *Computational Statistics and Data Analysis*, 53(8):2873–2884.

Fuentes, M. (2003). Statistical assessment of geographic areas of compliance with air quality standards. *Journal of Geophysical Research*, 108(D):9002.

Gelfand, A. E. and Smith, A. F. M. (1990). Sampling-based approaches to calculating marginal densities. *Journal of the American Statistical Association*, 85:398–409.

Genton, M. G. (2007). Separable approximations of space-time covariance matrices. *Environmetrics*, 18(7):681–695.

Gilleland, E. and Nychka, D. (2005). Statistical models for monitoring and regulating ground-level ozone. *Environmetrics*, 16(5):535–546.

Gramacy, R. B. and Apley, D. W. (2015). Local Gaussian process approximation for large computer experiments. *Journal of Computational and Graphical Statistics*, 24(2):561–578.

Gramacy, R. B., Bingham, D., Holloway, J. P., Grosskopf, M. J., Kuranz, C. C., Rutter, E., Trantham, M., and Drake, R. P. (2015). Calibrating a large computer experiment simulating radiative shock hydrodynamics. *Ann. Appl. Stat.*, 9(3):1141–1168.

Gramacy, R. B. and Lee, H. K. H. (2012). Cases for the nugget in modeling computer experiments. *Statistics and Computing*, 22(3):713–722.

Guhaniyogi, R., Finley, A. O., Banerjee, S., and Gelfand, A. E. (2011). Adaptive gaussian predictive process models for large spatial datasets. *Environmetrics*, 22(8):997–1007.

Hastings, W. K. (1970). Monte carlo sampling methods using markov chains and their applications. *Biometrika*, 57:97–109.

Henderson, H. V. and Searle, S. R. (1981). On deriving the inverse of a sum of matrices. *Siam Review*, 23(1):53–60.

Katzfuss, M. (2017). A multi-resolution approximation for massive spatial datasets. *Journal of the American Statistical Association*, 112(517):201–214.

Kaufman, C. G. and Shaby, B. A. (2013). The role of the range parameter for estimation and prediction in geostatistics. *Biometrika*, 100(2):473–484.

Konomi, B., Karagiannis, G., Sarkar, A., Sun, X., and Lin, G. (2014). Bayesian treed multivariate Gaussian process with adaptive design: Application to a carbon capture unit. *Technometrics*, 56(2):145–158.

Lindgren, F., Rue, H., and Lindström, J. (2011). An explicit link between Gaussian fields and Gaussian Markov random fields: the stochastic partial differential equation approach. *Journal of the Royal Statistical Society: Series B (Statistical Methodology)*, 73(4):423–498.

Ma, P. and Kang, E. L. (2017). Fused Gaussian process for very large spatial data. *arXiv:1702.08797*.

Mueller, P. (1993). Alternatives to the gibbs sampling scheme. Technical report, Institute Statistics and Decision Sciences, Duke University.

Nychka, D., Bandyopadhyay, S., Hammerling, D., Lindgren, F., and Sain, S. (2015). A multiresolution Gaussian process model for the analysis of large spatial datasets. *Journal of Computational and Graphical Statistics*, 24(2):579–599.

Nychka, D., Wikle, C., and Royle, J. A. (2002). Multiresolution models for nonstationary spatial covariance functions. *Statistical Modelling*, 2(4):315–331.

Oakley, J. and O’Hagan, A. (2002). Bayesian inference for the uncertainty distribution of computer model outputs. *Biometrika*, 89(4):769–784.

Peng, C.-Y. and Wu, C. F. J. (2014). On the choice of nugget in kriging modeling for deterministic computer experiments. *Journal of Computational and Graphical Statistics*, 23(1):151–168.

Rasmussen, C. E. and Williams, C. K. I. (2006). *Gaussian Processes for Machine Learning*. MIT Press, Cambridge, Mass.

Rougier, J. (2008). Efficient emulators for multivariate deterministic functions. *Journal of Computational and Graphical Statistics*, 17(4):827–843.

Sacks, J., Welch, W. J., Mitchell, T. J., and Wynn, H. P. (1989). Design and analysis of computer experiments. *Statistical Science*, 4(4):409–435.

Sang, H. and Huang, J. Z. (2012). A full scale approximation of covariance functions for large spatial data sets. *Journal of the Royal Statistical Society: Series B (Statistical Methodology)*, 74(1):111–132.

Stein, M. L., Chi, Z., and Welty, L. J. (2004). Approximating likelihoods for large spatial data sets. *Journal of the Royal Statistical Society: Series B (Statistical Methodology)*, 66(2):275–296.

van Dyk, D. A. and Jiao, X. (2015). Metropolis-Hastings Within Partially Collapsed Gibbs Samplers. *Journal of Computational and Graphical Statistics*, 24(2):301–327.

van Dyk, D. A. and Park, T. (2008). Partially Collapsed Gibbs Samplers. *Journal of the American Statistical Association*, 103(482):790–796.

Zhang, B., Konomi, B. A., Sang, H., Karagiannis, G., and Lin, G. (2015a). Full scale multi-output Gaussian process emulator with nonseparable auto-covariance functions. *Journal of Computational Physics*, 300(C):623–642.

Zhang, B., Sang, H., and Huang, J. Z. (2015b). Full-scale approximations of spatio-temporal covariance models for large datasets. *Statistica Sinica*, 25(1):99–114.